



LXR β is required for glucocorticoid-induced hyperglycemia and hepatosteatosis in mice

Rucha Patel,¹ Monika Patel,¹ Ricky Tsai,¹ Vicky Lin,^{2,3} Angie L. Bookout,^{2,4} Yuan Zhang,² Lilia Magomedova,¹ Tingting Li,² Jessica F. Chan,¹ Conrad Budd,¹ David J. Mangelsdorf,^{2,3} and Carolyn L. Cummins¹

¹Department of Pharmaceutical Sciences, University of Toronto, Toronto, Ontario, Canada. ²Department of Pharmacology, University of Texas Southwestern Medical Center, Dallas, Texas, USA. ³Howard Hughes Medical Institute, University of Texas Southwestern Medical Center, Dallas, Texas, USA. ⁴Department of Internal Medicine, Division of Hypothalamic Research, University of Texas Southwestern Medical Center, Dallas, Texas, USA.

Although widely prescribed for their potent antiinflammatory actions, glucocorticoid drugs (e.g., dexamethasone) cause undesirable side effects that are features of the metabolic syndrome, including hyperglycemia, fatty liver, insulin resistance, and type II diabetes. Liver x receptors (LXRs) are nuclear receptors that respond to cholesterol metabolites and regulate the expression of a subset of glucocorticoid target genes. Here, we show LXR β is required to mediate many of the negative side effects of glucocorticoids. Mice lacking LXR β (but not LXR α) were resistant to dexamethasone-induced hyperglycemia, hyperinsulinemia, and hepatic steatosis, but remained sensitive to dexamethasone-dependent repression of the immune system. In vivo, LXR α/β knock-out mice demonstrated reduced dexamethasone-induced expression of the key hepatic gluconeogenic gene, phosphoenolpyruvate carboxykinase (PEPCK). In perfused liver and primary mouse hepatocytes, LXR β was required for glucocorticoid-induced recruitment of the glucocorticoid receptor to the PEPCK promoter. These findings suggest a new avenue for the design of safer glucocorticoid drugs through a mechanism of selective glucocorticoid receptor transactivation.

Introduction

Glucocorticoids (GCs) and their synthetic analogs are among the most widely prescribed drugs in the world (1). GC drugs have profound antiinflammatory and immunosuppressive properties that are critical for the treatment of rheumatoid arthritis, cerebral edema, allergic reactions, asthma, and certain types of cancer. They are also employed as potent immunosuppressants to prevent organ transplant rejection and graft-versus-host disease (2). Unfortunately, the development of major metabolic side effects remains the key limitation for the long-term therapeutic use of GCs. Common side effects requiring dosage adjustment or cessation of treatment include diabetes, hypertension, osteoporosis, and muscle wasting (3).

GCs were first recognized as important determinants in diabetes when it was found that adrenalectomy of diabetic animals decreased hyperglycemia (4). Since then, there have been numerous reports linking elevated GCs with the metabolic syndrome, obesity, and insulin resistance (5–9). Patients with Cushing syndrome (a rare condition characterized by elevated endogenous GCs) develop an abnormal fat distribution, insulin resistance, hyperglycemia, and hypertension in 80%–90% of cases (10). Fatty liver (hepatic steatosis) has also been characterized in Cushing patients (11), and several studies have found that hepatic steatosis is an independent risk factor for the development of insulin resistance (12–15).

The role of endogenous GCs is to supply the body with enough glucose to survive under conditions of acute stress or reduced glucose intake. The physiologic response to stress is mediated by the release of cortisol (in humans) or corticosterone (in rodents) into the bloodstream. The increase in GC hormone then acts on multiple metabolic tissues via its receptor to increase circulating glucose levels.

The mechanisms by which GCs achieve this effect are multifactorial and involve the following: (a) increased hepatic glucose production (gluconeogenesis) (16), (b) decreased peripheral glucose uptake into muscle and adipose (17, 18), (c) breakdown of muscle and fat to provide additional substrates for glucose production (19, 20), and (d) inhibition of insulin release from pancreatic β cells (9, 21). The stress response is intended to be of short duration to reset the balance of plasma glucose. If prolonged GC exposure is present (as with therapeutic use of GCs or in Cushing syndrome), insulin secretion will increase to compensate for the excess glucose and ultimately result in severe insulin resistance and metabolic dysfunction.

The GC receptor (GR) and liver X receptors LXR α (NR1H3) and LXR β (NR1H2) are members of the nuclear receptor superfamily of transcription factors that regulate distinct but overlapping transcriptional programs (22, 23). GR and LXR β are expressed at relatively high levels throughout the body, whereas LXR α expression is highest in liver, kidney, intestine, adipose, and adrenal gland (24). GCs act by binding to GR in the cytoplasm, causing translocation of the ligand-bound receptor to the nucleus. There, GR homodimerizes and activates the carbohydrate metabolic pathway through the direct binding and activation of GR response elements in key gluconeogenic enzymes such as phosphoenolpyruvate carboxykinase (PEPCK) and glucose-6-phosphatase (G6Pc) (25, 26). In addition, activation of GR represses the expression of several genes involved in inflammation (e.g., IL-1, TNF- α , IL-6, and COX-2), a function that accounts for the widespread therapeutic use of synthetic GCs. The endogenous ligands of LXRs are oxidative metabolites of cholesterol, also called oxysterols. As such, the LXRs are known for their important role in modulating whole-body cholesterol homeostasis by acting as sensors of the intracellular cholesterol load (27, 28). Upon activation, LXR increases the expression of an array of genes involved in cholesterol efflux (29–31), cholesterol metabolism (32, 33), and fatty acid synthesis (34). Interestingly, like GR, LXRs have potent

Authorship note: Rucha Patel and Monika Patel contributed equally to this work.

Conflict of interest: David J. Mangelsdorf has ownership in stock of Ligand Pharmaceuticals and is a consultant for Reset Therapeutics.

Citation for this article: *J Clin Invest.* 2011;121(1):431–441. doi:10.1172/JCI41681.

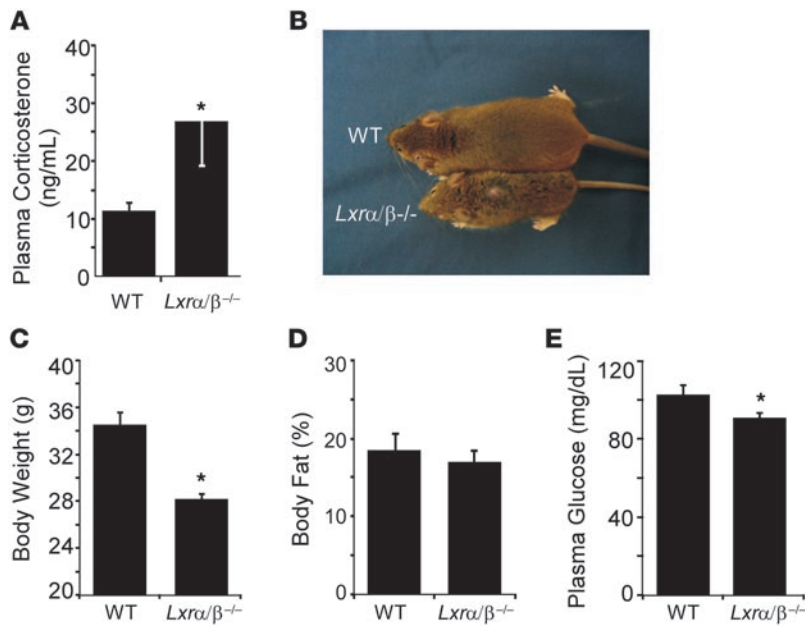


Figure 1

Lxra/β^{-/-} mice are hypercorticosteronemic but do not exhibit symptoms of Cushing syndrome. (A) Circulating corticosterone from WT and *Lxra/β^{-/-}* mice ($n = 4$) measured at the peak of the circadian rhythm (10 pm, 2 hours after lights off). Plasma was analyzed for corticosterone level by LC/MS/MS. (B) Size comparison of 15-month-old male WT and *Lxra/β^{-/-}* mice. The size differential between the genotypes is most pronounced after 1 year of age. (C) Body weights of WT ($n = 17$) and *Lxra/β^{-/-}* ($n = 36$) mice at 6 months of age. Body fat (D) and plasma glucose (E) levels from WT and LXR-null mice measured by NMR minispec and tail nick, respectively (average ± SEM, $n = 10$). Mice used in C–E were male mice (6 month) fed a chow diet. * $P < 0.05$ versus WT (Student's *t* test).

antiinflammatory actions that are due to repression of a number of overlapping target genes (35). However, in contrast to GR, activation of LXR α has been shown to have beneficial effects in diabetic rodent models by improving glucose control (36–38). This improvement has been attributed to inhibition of hepatic PEPCK (37, 38), G6Pc (38, 39), and 11 β -hydroxysteroid dehydrogenase (40); and increased skeletal GLUT4 expression (38, 41), collectively resulting in decreased circulating glucose.

Taken together, the studies above highlight striking parallels between the genes regulated by GR and LXR. Recently, we showed that circulating GCs (corticosterone) are elevated in *Lxra/β^{-/-}* mice (42). This hypercorticosteronemia correlated with a basal derepression of the LXR α -target gene steroidogenic acute regulatory protein (StAR), which is rate limiting for GC synthesis from cholesterol. Intriguingly, despite having higher circulating GCs, the *Lxra/β^{-/-}* mice did not exhibit hallmarks of GC excess, such as obesity and insulin resistance. In this study, we investigated whether there was a functional requirement for LXR in eliciting the metabolic effects of exogenous GC administration. Here, we demonstrate that LXR β is required for the development of GC-mediated hyperglycemia and hepatic steatosis, but not GC-mediated antiinflammatory effects.

Results

Lxra/β^{-/-} mice exhibit hypercorticosteronemia without Cushing disease symptoms. We previously reported that *Lxra/β^{-/-}* mice develop adrenomegaly and have 2-fold higher basal morning corticosterone levels in plasma compared with WT mice (42). These basal differences persist throughout the circadian cycle because corticosterone levels remained 2-fold higher in *Lxra/β^{-/-}* mice compared with WT mice in the evening (Figure 1A). In agreement with our previous work (43), *Lxra/β^{-/-}* mice were lean (Figure 1, B and C) and had a percentage of fat similar to that of WT mice (Figure 1D). In addition, *Lxra/β^{-/-}* mice had lower fasting glucose levels compared with WT mice (Figure 1E).

Lxra/β^{-/-} mice are resistant to GC-induced hyperglycemia. To determine whether *Lxra/β^{-/-}* mice are resistant to the metabolic effects of elevated GCs, we treated WT and *Lxra/β^{-/-}* mice with dexamethasone (DEX) or vehicle for 5 days and sacrificed the animals on day 6. DEX was chosen for these studies because it is a potent GR agonist with insignificant mineralocorticoid receptor activity and has been well studied in humans and animals. As expected, the DEX-treated WT mice developed hyperglycemia (3-fold increase in circulating glucose compared with vehicle), whereas DEX-treated *Lxra/β^{-/-}* mice were

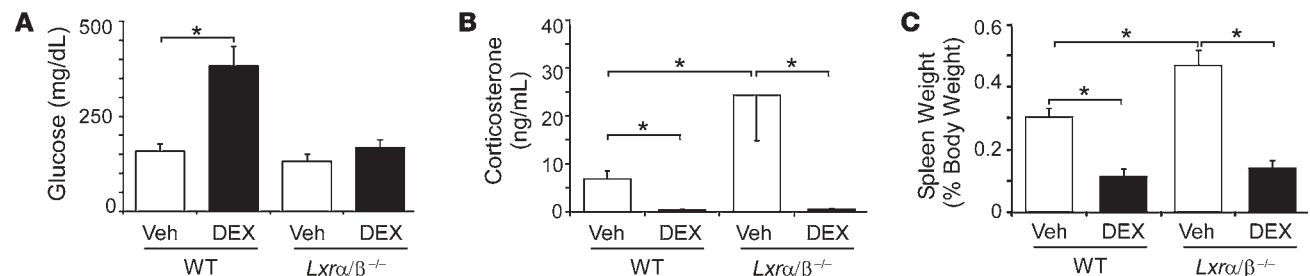
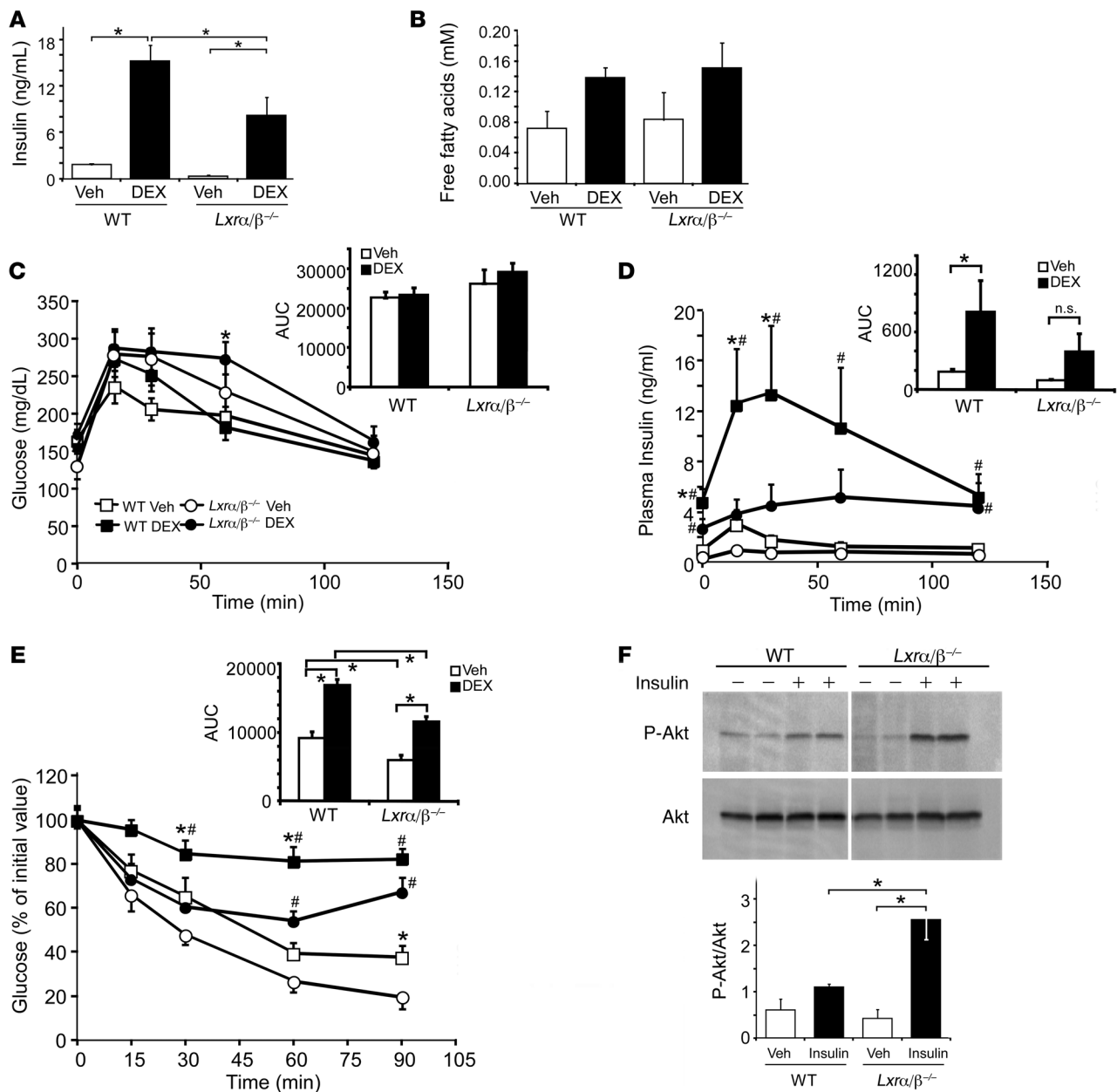


Figure 2

Lxra/β^{-/-} mice display dissociated GC effects. WT and *Lxra/β^{-/-}* mice (6 months, male) were treated with 2.5 mg/kg DEX or vehicle (sesame oil) twice a day for 5 days (A and B) or 14 days (C). Mice were sacrificed by decapitation at lights on in the fed state. Trunk blood was collected, and organs were harvested. Plasma glucose (A) and plasma corticosterone (B) levels were measured using commercial kits. (C) The spleen weight was used as a marker of lymphoid organ atrophy. Data shown represent average ± SEM, $n = 4–6$. * $P < 0.05$ by ANOVA and Student-Newman-Keuls.

**Figure 3**

Insulin tolerance is maintained in DEX-treated *Lxra/β^{-/-}* mice. (A and B) WT and *Lxra/β^{-/-}* mice were treated with DEX or vehicle for 5 days. Plasma insulin (A) and free fatty acids (B) were measured in the fed state using commercially available kits. (C–E) Mice were treated with DEX or vehicle for 7 days and fasted for 4 hours prior to performing the OGTT (C, D) and ITT (E) tests. (C and D) Mice were gavaged with 20% D-glucose (2 g/kg) and blood sampled from a tail nick at different time points. Plasma glucose (C) was assayed using a colorimetric kit, and plasma insulin (D) from the glucose tolerance test was assayed by RIA. (E) Insulin was injected i.p. at 0.75 U/kg, and plasma was assayed at regular intervals to measure glucose. The definitions of circles and squares in part C also apply to parts D and E. Mice were injected with saline or insulin (1.5 U/kg, i.p.) 5 minutes prior to sacrifice. Liver extracts (20 μg) were immunoblotted using antibodies against p-Akt and normalized against total Akt (F). Samples were run on the same gel but were noncontiguous. Data shown are average ± SEM. $n = 4$ (A and B); $n = 7$ (C and D); $n = 6–7$ (E). * $P < 0.05$, ANOVA followed by Student-Newman-Keuls. In line graphs C–E, asterisks indicate significant difference from *Lxra/β^{-/-}* mice with the same treatment regimen. # $P < 0.05$, ANOVA followed by Student-Newman-Keuls, significantly different from vehicle-treated control of same genotype.

refractory to this effect (Figure 2A). Notably, *Lxra/β^{-/-}* mice were still sensitive to feedback repression of corticosterone by DEX (Figure 2B). Spleen weight was measured as a secondary marker of immune function, since lymphoid organ atrophy is commonly observed after chronic GC treatment. Both WT and *Lxra/β^{-/-}* mice exhibited signifi-

cant atrophy of the spleen with chronic DEX treatment (Figure 2C). Thus, the *Lxra/β^{-/-}* mice represent a unique animal model that exhibits dissociated GC actions (i.e., resistance to the glycemic response of DEX but sensitive to feedback repression of the hypothalamic-pituitary-adrenal (HPA) axis and lymphoid organ atrophy).

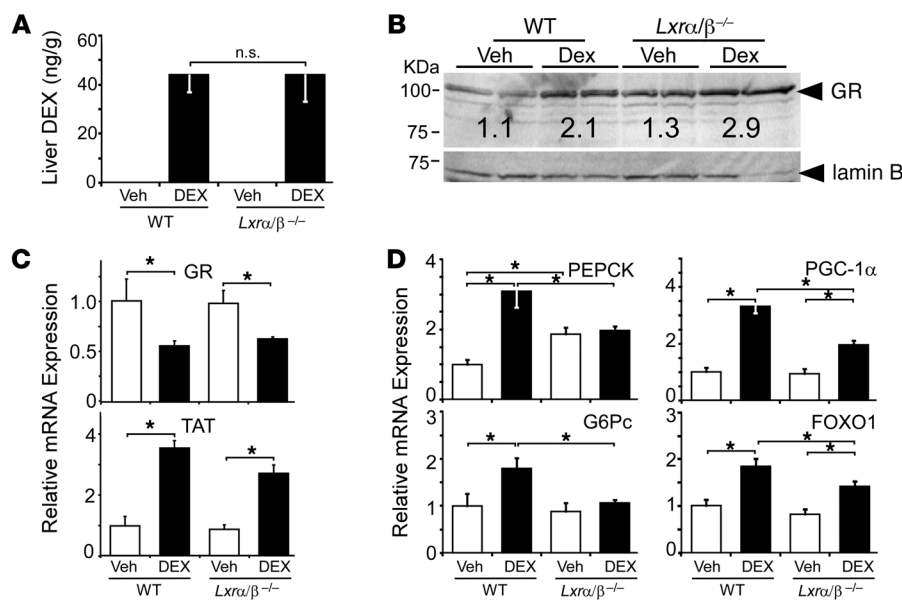
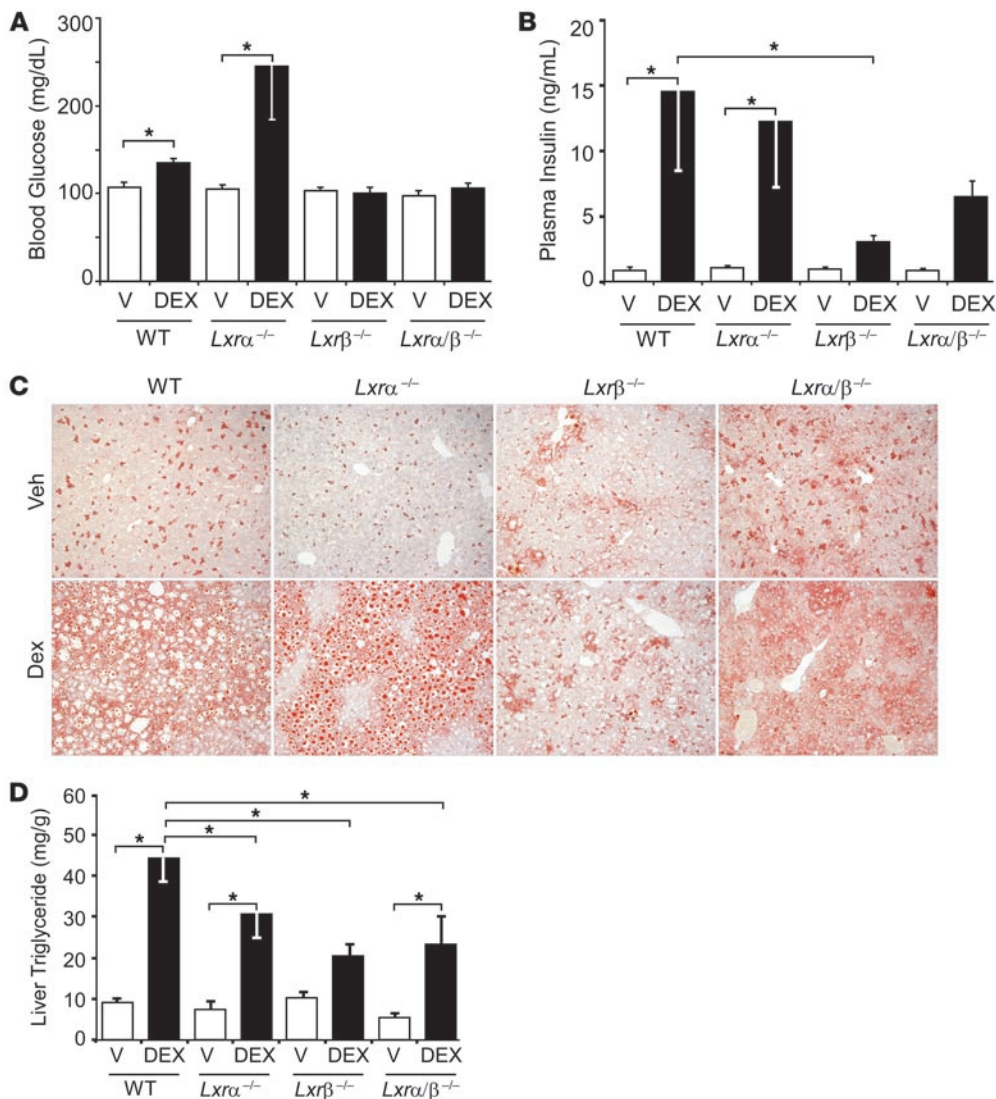


Figure 4 Selective regulation of GR target genes in *Lxra/β^{-/-}* mice treated with DEX. WT and *Lxra/β^{-/-}* mice (6 months, male) were treated with 2.5 mg/kg DEX or vehicle (sesame oil) b.i.d. for 5 days. (A) Organic extracts of liver (~100–200 mg) were analyzed by LC/MS/MS for intra-hepatic DEX levels after chronic treatment with DEX (average ± SEM, *n* = 5). (B) Expression of GR from liver nuclear extracts of mice treated with DEX. Protein (40 μg/lane) was normalized for loading using the nuclear marker lamin B. Values represent the average GR protein level normalized to lamin B. (C and D) Real-time QPCR was performed on liver RNA. Gene expression changes were calculated using the comparative Ct method with cyclophilin as the reference gene and WT, vehicle as the calibrator. Samples exhibit non-LXR-selective and LXR-selective changes in gene expression (average ± SEM). *n* = 4–6 (C); *n* = 8–11 (D). **P* < 0.05 by ANOVA and Student-Newman-Keuls.

Lxra/β^{-/-} mice are refractory to DEX-induced insulin intolerance. To further investigate the role of LXRs in the DEX-mediated effects on carbohydrate metabolism, circulating insulin levels and insulin tolerance were assessed. As expected, insulin levels increased dramatically in response to DEX-induced hyperglycemia in WT and *Lxra/β^{-/-}* mice (Figure 3A). However, insulin levels remained lower in *Lxra/β^{-/-}* mice treated with DEX relative to WT mice. As previously reported (43), *Lxra/β^{-/-}* mice also had lower basal levels of insulin compared with WT mice (Figure 3A). There were no significant differences in plasma free fatty acids between WT and *Lxra/β^{-/-}* mice treated with DEX (Figure 3B), although there was a trend toward increased levels with DEX, consistent with previous studies (44). Glucose and insulin tolerance tests (ITTs) were performed on WT and *Lxra/β^{-/-}* mice after a 7-day treatment with DEX. A trend toward decreased glucose tolerance was seen in both WT and *Lxra/β^{-/-}* mice treated with DEX compared with mice that received vehicle (Figure 3C), consistent with the known effects of DEX on decreasing peripheral insulin sensitivity (9). Although there was no significant difference in plasma glucose between *Lxra/β^{-/-}* and WT mice during the glucose tolerance test, plasma insulin levels were markedly higher in WT animals treated with DEX (Figure 3D), demonstrating that LXR-null mice required less absolute levels of insulin to achieve a similar level of glucose excursion. Furthermore, under both basal and chronic DEX treatment, there was significant preservation of insulin tolerance in the *Lxra/β^{-/-}* mice compared with WT mice, especially at the early time points (15 and 30 minutes) but also over the entire time course as assessed by AUC (Figure 3E). This suggested that the enhanced insulin tolerance in the *Lxra/β^{-/-}* mice favorably contributes to the prevention of hyperglycemia under chronic DEX treatment. In support of this conclusion, we noted that the level of hepatic phosphorylated Akt (normalized to total Akt) was enhanced 2.5-fold in *Lxra/β^{-/-}* mice relative to WT mice after 5 minutes exposure to i.p. insulin (Figure 3F). Taken together, these data demonstrate that *Lxra/β^{-/-}* mice remain more insulin tolerant compared with WT mice when challenged with DEX, despite having similar plasma FFA levels.

Lxra/β^{-/-} mice differentially activate GR target genes in liver. To determine whether the selective effects of DEX observed in the *Lxra/β^{-/-}* mice were due to differential expression or activation of GR, DEX and GR levels were measured in the liver. There was no significant difference in the hepatic exposure to DEX in WT and *Lxra/β^{-/-}* as measured by liquid chromatography tandem mass spectrometry (LC/MS/MS) (Figure 4A). In addition, the translocation of GR from the cytoplasm to the nucleus in response to ligand was intact, since GR nuclear protein levels remained similar in livers of WT and *Lxra/β^{-/-}* mice treated with DEX (Figure 4B). Furthermore, GR mRNA levels were unchanged between WT and *Lxra/β^{-/-}*, and DEX treatment decreased GR mRNA significantly in the liver of both genotypes (Figure 4C). Consistent with these findings, the classic GR target gene tyrosine aminotransferase (TAT) (45, 46) was induced to a similar extent in WT and *Lxra/β^{-/-}* mice (Figure 4C). Remarkably, expression of PEPCK and G6Pc was differentially induced in WT versus *Lxra/β^{-/-}* animals. In agreement with known regulation by GR, DEX increased PEPCK expression 3-fold and G6Pc expression 1.8-fold in WT mice but not in *Lxra/β^{-/-}* mice (Figure 4D). Analysis of PGC-1α and FOXO1, 2 other known transcriptional regulators of PEPCK and G6Pc, showed DEX-dependent increases in their expression in WT mice (Figure 4D). In *Lxra/β^{-/-}* mice, DEX still induced expression of FOXO1 and PGC-1α, but this induction was diminished significantly compared with WT mice. Together, these data point to a role for LXR in modulating gene-selective GR activation.

Lxra/β^{-/-} mice are protected from GC-induced hyperglycemia and hyperinsulinemia. To explore the contribution of the 2 LXR proteins to the selective hepatic GC resistance, *Lxra^{-/-}* and *Lxrβ^{-/-}* mice were subjected to chronic DEX administration and phenotypic characterization was performed. LXRα is regarded as the most active LXR isoform in the liver because of its high expression and critical role in the regulation of lipogenesis and cholesterol homeostasis (33, 47–50). Interestingly, after 14 days of DEX treatment, resistance to hyperglycemia was only observed in *Lxrβ^{-/-}* and *Lxra/β^{-/-}* mice, and not in WT or *Lxra^{-/-}* mice (Figure 5A). Consistent with these data, the WT and *Lxra^{-/-}* mice became severely hyperinsulinemic after DEX treatment (Figure 5B). In oral glucose tolerance tests (OGTTs), *Lxra^{-/-}* mice were less

**Figure 5**

Lxrβ^{-/-} mice are resistant to developing GC-induced hyperglycemia, hyperinsulinemia, and hepatic steatosis. WT, *Lxra*^{-/-}, *Lxrβ*^{-/-}, and *Lxra/β*^{-/-} mice were treated with DEX (2.5 mg/kg, b.i.d.) or vehicle (V) for 14 days (by i.p. injection). (A) Blood glucose levels were measured by tail nick 6 hours after lights on in fed mice using a handheld glucometer **P* < 0.05, *t* test. (B) Plasma insulin was measured using a sensitive rat insulin RIA kit. (C) Liver sections were stained with oil red O and examined under brightfield microscopy. Original magnification, ×100 (representative image from *n* = 3/treatment group). Preweighed liver sections were homogenized in chloroform/methanol (2:1) and lipids extracted by the Folch method. Dried aliquots were assayed for liver triglycerides (D) using a commercial kit. Average ± SEM. *n* = 4–6 (A, B, and D). **P* < 0.05, ANOVA followed by Student-Newman-Keuls.

glucose tolerant after DEX treatment relative to vehicle (measured by the AUC), whereas *Lxrβ*^{-/-} mice actually had improved glucose tolerance after DEX (Supplemental Figure 1A; supplemental material available online with this article; doi:10.1172/JCI41681DS1). Furthermore, the corresponding insulin levels were dramatically increased in the *Lxra*^{-/-} mice treated with DEX (Supplemental Figure 1B), reminiscent of the response seen in WT mice (Figure 3D). In contrast, this insulin response was severely dampened after a glucose bolus in the DEX-treated *Lxrβ*^{-/-} mice (Supplemental Figure 1B). These data suggest that, similar to the *Lxra/β*^{-/-} mice, the *Lxrβ*^{-/-} mice require less absolute levels of insulin to achieve a similar level of glucose excursion. In addition, the insulin data are consistent with a previous report that demonstrated that islets isolated from *Lxrβ*^{-/-} mice exhibited decreased glucose-stimulated insulin secretion (51).

Taken together, the glucose and insulin profiles after OGTT suggest that the *Lxra*^{-/-} mice are potentially more susceptible to developing GC-induced hyperglycemia than WT mice. Consistent with this notion, activation of LXRα by synthetic LXR agonists has been shown to reverse hyperglycemia in mouse models of insulin resistance (37, 38). Therefore, loss of the protective effect of LXRα under these conditions would be expected to result in an exacerbation of the GC effect.

Lxrβ^{-/-} mice are protected from GC-induced hepatic steatosis. The development of insulin resistance is highly correlated with the presence of fatty liver. We explored whether the preserved glucose tolerance in the *Lxrβ*^{-/-} and insulin tolerance in the *Lxra/β*^{-/-} mice after DEX treatment correlated with decreased fat accumulation in the liver. Histologic examination of liver sections was performed with oil red O staining to detect neutral lipids. Significant lipid droplets were observed in livers of WT and *Lxra*^{-/-} mice treated with DEX, whereas no change was detected in the liver histology of *Lxrβ*^{-/-} and *Lxra/β*^{-/-} mice between vehicle and DEX treatment (Figure 5C). Liver triglyceride levels were significantly increased with DEX in all genotypes except *Lxrβ*^{-/-}, although the same trend was observed in this genotype (Figure 5D). These data correlate strongly with the insulin levels measured after DEX treatment (Figure 5B), supporting the essential role of insulin in the development of GC-induced hepatic steatosis (52, 53).

Recruitment of GR to its target genes is decreased in livers of Lxrβ^{-/-} and *Lxra/β*^{-/-} mice. To determine whether the requirement for LXRs in the GC regulation of PEPCK was autonomous to the liver, gene expression was investigated in primary mouse hepatocytes. PEPCK was selectively induced by DEX in WT and *Lxra*^{-/-} but not

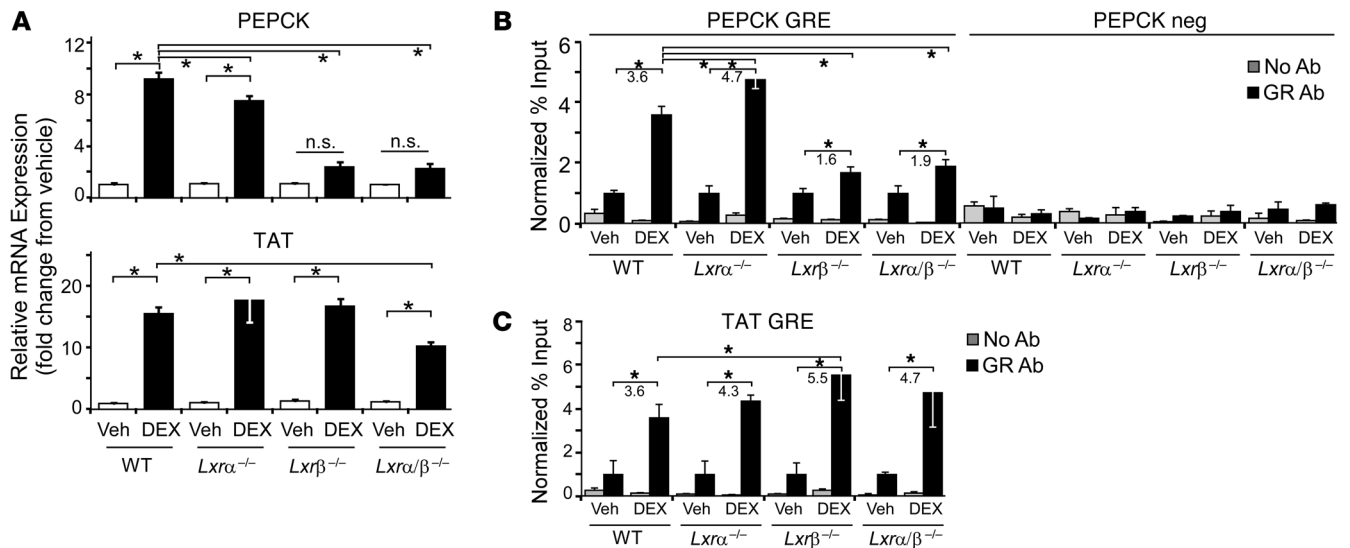


Figure 6 Recruitment of GR to the PEPCK promoter is decreased in livers of $Lxr\beta^{-/-}$ and $Lxra/\beta^{-/-}$ mice. **(A)** Primary hepatocytes were seeded on 6-well collagen-coated plates and treated with vehicle (DMSO) or DEX (10 nM) for 16 hours. RNA was extracted, reverse transcribed, and analyzed for gene expression by real-time QPCR. Data pooled from 2 independent experiments (average \pm SEM, $n = 5-6$). **(B and C)** ChIP of GR protein from mice perfused with vehicle or 10 nM DEX through the portal vein for 30 minutes. The negative control region for PEPCK was at -3 kb relative to the transcription start site. Chromatin was pooled from 2 mice per treatment, and results are expressed relative to percentage of input and normalized to GR vehicle (Veh) for each genotype. Error bars represent PCR amplification variability (average \pm SD, $n = 3$). The values for the GR Ab PEPCK and TAT GREs prior to normalization were as follows: WT (0.08, 0.05); $Lxra^{-/-}$ (0.06, 0.08); $Lxr\beta^{-/-}$ (0.06, 0.02); $Lxra/\beta^{-/-}$ (0.08, 0.02). * $P < 0.05$ ANOVA and Student-Newman-Keuls. Fold changes are indicated on the graphs.

in $Lxr\beta^{-/-}$ and $Lxra/\beta^{-/-}$ primary hepatocytes (Figure 6A). In contrast, the induction of TAT was similar in all genotypes. Two additional GCs were tested (cortisol and triamcinolone acetonide) in primary hepatocytes and showed the same result, demonstrating that this effect is not DEX specific but represents a general GC-mediated effect (data not shown). These data indicate a hepatocyte autonomous role for LXR in contributing to GC-induced hepatic gluconeogenesis.

To address the mechanism of these promoter-specific actions of GCs, we next investigated promoter occupancy by in vivo chromatin immunoprecipitation of GR bound to the GC response element (GRE) of either the PEPCK or the TAT gene promoters. As expected, there was a robust recruitment of GR to both the PEPCK and TAT GREs in response to DEX treatment in WT mice (Figure 6, B and C). Remarkably, GR occupancy of the PEPCK promoter, but not the TAT promoter, was dramatically decreased in the $Lxr\beta^{-/-}$ and $Lxra/\beta^{-/-}$ mice in response to DEX. These data strongly support the notion that LXR β is required for the selective binding of GR to the PEPCK promoter.

The immunosuppressive effects of DEX are maintained in LXR-null mice. GCs are widely used therapeutically for their immunosuppressive and antiinflammatory effects. Since hepatic steatosis and hyperglycemia were differentially induced in the $Lxr\beta^{-/-}$ mice in response to DEX, it was of interest to determine whether the anti-inflammatory response to GCs was preserved. Examination of the lymphoid tissues and white blood cells from LXR-null mice treated with DEX for 14 days confirmed that the loss of LXR β does not influence the ability of GCs to suppress the immune response (as previously shown for $Lxra/\beta^{-/-}$ mice in Figure 1C). Spleen atrophy was apparent in both $Lxra^{-/-}$ and $Lxr\beta^{-/-}$ mice (Figure 7A). A differential white cell count definitively demonstrated that lymphocyte

extravasation and neutrophil demargination were present with DEX treatment regardless of the LXR genotype (Figure 7B). To directly assess the molecular effects of DEX on the immune system, we measured the mRNA expression of cytokines from thioglycolate-elicited peritoneal macrophages. As expected, after stimulation with LPS, there was a significant increase in the expression of key proinflammatory cytokines such as IL-1 β , IL-6, and TNF- α from the primary macrophages (Figure 7C). The response to LPS in the $Lxra^{-/-}$, $Lxr\beta^{-/-}$, and $Lxra/\beta^{-/-}$ macrophages was attenuated compared with that of the WT mice. These data are consistent with both LXR isoforms playing a role in the immune response and support previous reports that $Lxra/\beta^{-/-}$ mice are more susceptible to infection than WT mice (54-56). In addition, pretreatment with DEX dramatically decreased the cytokine expression in response to LPS for all LXR genotypes (Figure 7C). Therefore, while there is an LXR β -dependent GC response in the liver on glucose metabolism, the response to GCs in the immune system appears to be independent of LXR.

Discussion

In this report, we detail the discovery of LXR β as an important potentiating factor in GC-mediated hyperglycemia and hepatic steatosis. As discussed below, these findings are of both physiologic and pharmacologic interest. On the physiologic side, this work reveals an unexpected crosstalk between LXR and GC regulation of glucose and lipid metabolism. GCs potently upregulate hepatic glucose production under conditions of stress to protect the body from excessive nutrient depletion. This outcome is achieved through the upregulation of numerous genes in the gluconeogenic pathway that include PEPCK and G6Pc. PEPCK is considered to be the rate-limiting enzyme in gluconeogenesis and

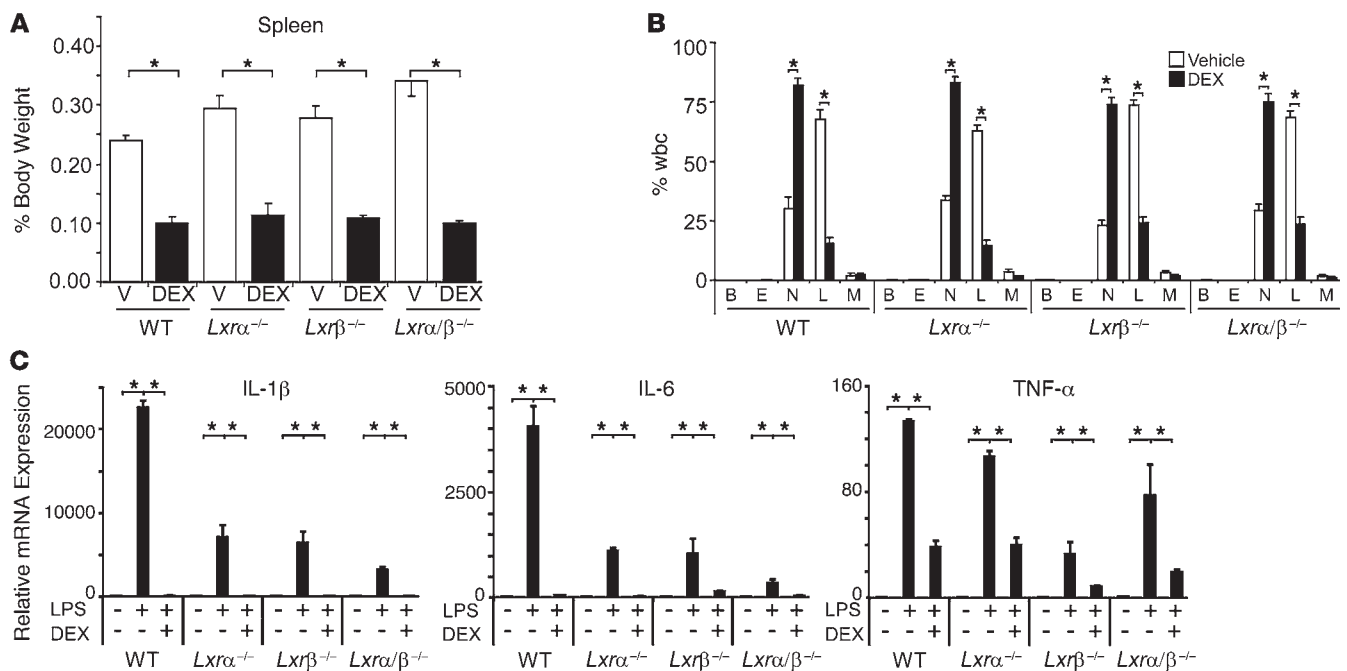


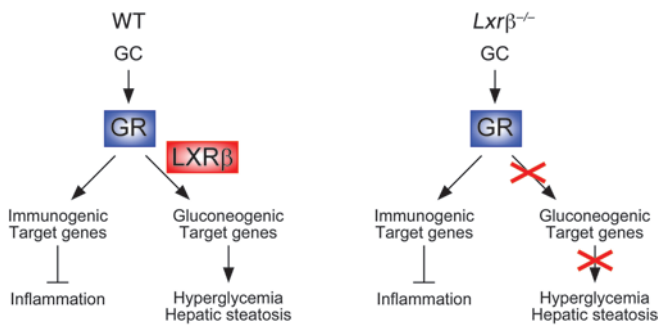
Figure 7

Lxrβ^{-/-} mice remain sensitive to the immunosuppressive effects of DEX. (A) WT, *Lxra*^{-/-}, *Lxrβ*^{-/-}, and *Lxra/β*^{-/-} mice were treated with DEX (2.5 mg/kg, b.i.d.) for 14 days (by i.p. injection). The spleen was weighed at the time of sacrifice using an analytical balance. (B) Blood smears were obtained 6 days after initiating DEX treatment by tail nick. After staining, a differential white blood cell count was performed under ×40 magnification. B, basophils; E, eosinophils; N, neutrophils; L, lymphocytes; M, monocytes. (C) Thioglycolate-elicited peritoneal macrophages were treated with vehicle or 100 nM DEX (6 hours) followed by LPS stimulation (10 ng/ml) for an additional 18 hours. RNA was extracted, reverse transcribed, and analyzed for gene expression by real-time QPCR. Average ± SEM, *n* = 4–6 (A and B); average ± SD, *n* = 3 (C). **P* < 0.05, Student's *t* test for comparison of groups within 1 genotype.

as such the molecular factors controlling the expression of this gene have been extensively studied (25, 57–62). PEPCK transcription is strongly activated by GCs and inhibited by insulin (63). In addition to GR, numerous proteins are bound to accessory factor sites on the PEPCK promoter either directly or indirectly and are essential for maximal GC response including PPARα (64), FOXO1 (65), and PGC1α (65). We found the induction of liver PEPCK, FOXO1, and PGC1α after DEX treatment was significantly attenuated in the *Lxra/β*^{-/-} mice compared with WT mice. In addition, *Lxra/β*^{-/-} mice remained more insulin tolerant than WT mice after chronic DEX treatment determined from basal insulin values and an ITT, and this effect was specifically due to loss of LXRβ. From experiments performed in primary hepatocytes, we found that the selective transcriptional effect of GCs was cell autonomous and required LXRβ despite the fact that the enhanced insulin tolerance of the *Lxra/β*^{-/-} mice would also contribute to protection against GC-induced hyperglycemia. Together, these data suggest that LXRβ in the liver contributes selectively to the regulation of key gluconeogenic enzymes including PEPCK.

Nonalcoholic fatty liver results from an imbalance of fat metabolism in the liver. This can arise if there is excessive fatty acid uptake or synthesis, decreased fatty acid oxidation, or decreased secretion of VLDL particles. GCs are known to contribute to fatty liver production through a combination of increased fatty acid synthesis and decreased fatty acid β oxidation (66). The effect of GCs on promoting fatty acid synthesis has been shown to require the presence of insulin. In fact, GCs alone, in the absence of insulin, do not

promote fatty acid synthesis (53). However, when combined with insulin, GCs synergistically increase de novo lipogenesis (52). While extensive studies have been performed to understand the molecular regulation of gluconeogenesis by GCs (61), the detailed molecular mechanisms by which GCs induce fatty liver have not been well characterized (9). It was recently reported that downregulation of the transcriptional repressor HES1 by GR is important in promoting fatty liver because reconstitution of HES1 promoted lipolysis through the ectopic expression of pancreatic lipases (67). These same lipases were recently reported to be upregulated by PPARα activation (68). Our data suggest that this mechanism is not involved in the resistance to fatty liver seen in the *Lxra/β*^{-/-} mice since the expression of HES1 was not significantly altered by DEX and we were unable to detect the expression of these pancreatic lipases in our liver samples (Supplemental Figure 2 and data not shown). PPARα, a key transcriptional regulator of fatty acid oxidation, has been found to be essential for DEX-mediated induction of hypertension and insulin resistance in *Ldlr*^{-/-}*Ppara*^{-/-} animals, but its role in hepatic steatosis was not analyzed in that study (69). Here, we found that PPARα expression was unchanged between WT and *Lxra/β*^{-/-} mice and downstream target genes were not dramatically or differentially altered with DEX in WT and *Lxra/β*^{-/-} mice (Supplemental Figure 2). PPARγ has been recently implicated in hepatic steatosis through the regulation of fat-specific protein 27 (FSP27), a direct PPARγ target gene (70). In our study, PPARγ expression itself was not significantly changed by DEX in both WT and *Lxra/β*^{-/-} mice, whereas FSP27 was induced equally by DEX in WT and

**Figure 8**

Selective activation of the hepatic GC-response pathway. LXR β is modulating the GC-dependent induction of hyperglycemia and hepatic steatosis by increasing hepatic glucose production and decreasing glucose tolerance, contributing to insulin resistance and diabetes. Lxr $\beta^{-/-}$ (and Lxr $\alpha/\beta^{-/-}$) mice remain sensitive to the immunologic effects of GCs.

Lxr $\alpha/\beta^{-/-}$ mice, suggesting this pathway was not involved in selective fatty liver production (Supplemental Figure 2). The transcription factor SREBP-1c has been previously shown to be critical for inducing an overall program of lipogenesis and promoting fatty liver (71). As expected, due to the known direct regulatory effect of LXR α on SREBP-1c expression (48, 72), basal expression of SREBP-1c was greatly decreased in Lxr $\alpha/\beta^{-/-}$ mice (Supplemental Figure 2). However, DEX actually decreased the expression of SREBP-1c in WT mice, suggesting that this pathway cannot account for the increased fatty liver seen in WT mice treated with DEX. In summary, the mechanism by which the LXR β and LXR α/β knockout mice are protected from fatty liver appears to be independent of the known pathways affected by GC regulation. This is the first LXR β -specific role that has been ascribed in the liver, an organ in which LXR α has been recognized as the critical mediator of both cholesterol metabolism and lipogenesis. A plausible hypothesis that is the subject of future studies is that the LXR β effects on hepatic steatosis may be related to the enhanced glucose tolerance in the Lxr $\beta^{-/-}$ mice after chronic DEX treatment (Supplemental Figure 1A).

GCs mediate their antiinflammatory effects through the differential tethering of GR to individual transcription factors such as NF- κ B and c-Jun (73, 74). The transrepressive effects of GCs are primarily responsible for the beneficial therapeutic effects on the immune system (for example, repression of IL-6 and TNF- α). Transactivation of GR is believed to be responsible for the negative side effects of therapeutic GCs including hyperglycemia (PEPCK, G6Pc), muscle catabolism (myostatin, glutamine synthetase), and osteoporosis (receptor activator of NF- κ B ligand) (75). As such, the pharmaceutical industry has been interested in developing “dissociated” GR agonists that can separate the transrepression from transactivation activities (76, 77). This strategy has provided successful novel steroidal candidates *in vitro*, but the effects have not faithfully translated *in vivo*. More recent compounds with a nonsteroidal structure have begun to be used *in vivo* with an enhanced side effect profile compared with steroidal ligands (78). Complicating the application of the dissociated ligand strategy are genes that are transactivated by GR but critical for its antiinflammatory effects such as MAPK phosphatase 1 (MKP-1) and GC-induced leucine zipper (GILZ) (75). The finding that LXR β selectively promotes gene-specific transactivation opens a new avenue for the development of GC-selective ligands that does not depend on separating transactivation from transrepression.

To capitalize on the discovery that LXR β is potentiating some of the negative metabolic effects of GCs, a detailed molecular mechanism for how selective transactivation occurs must be uncovered. While an improved insulin tolerance in LXR α/β -null mice would provide protection against DEX-induced hyperglycemia, the cell autonomous effect of PEPCK regulation in the primary hepatocytes suggests a more direct mechanism is involved. We have shown that the GC levels in the livers of WT and Lxr $\alpha/\beta^{-/-}$ mice treated with DEX are similar, yet there is differential regulation of GR target genes that points to a promoter-specific mechanism. To that end, we have shown that GR is differentially recruited to the PEPCK promoter in the absence of LXR. This effect is not due to a general decrease in recruitment of cofactors to the PEPCK promoter in the Lxr $\alpha/\beta^{-/-}$ mice since 2 other factors important for PEPCK activation (C/EBP β and SRC-1) were similarly recruited (Supplemental Figure 3). Coimmunoprecipitation studies in HEK293 cells overexpressing GR and Flag-tagged LXR α or LXR β uncovered an interaction between GR and each isoform of LXR (our unpublished observations). Therefore, this protein-protein interaction is unlikely to account for the LXR β -specific mechanism demonstrated herein unless competition is occurring between the 2 receptors for binding to GR. Ongoing studies are currently being directed at understanding the basis for the selective recruitment of GR to the PEPCK promoter. In addition, it will be of interest to explore whether other detrimental effects of long-term GCs, including osteoporosis and muscle wasting, show LXR selectivity.

In summary, the discovery that the Lxr $\alpha/\beta^{-/-}$ mice were hypercorticosteronemic without exhibiting Cushing-like symptoms prompted our investigation into whether the mice were resistant to the effects of GCs. Through the use of the potent synthetic ligand DEX, we discovered that Lxr $\alpha/\beta^{-/-}$ mice were selectively resistant to some of the effects of GCs — most notably the metabolic effects — but were still sensitive to the immunosuppressive effects (Figure 8). Furthermore, we uncovered the liver as a key organ influencing the effect of LXR β on GC-mediated induction of PEPCK. The data presented herein renew the optimism that a more selective GC agonist can be designed to provide exceptional antiinflammatory action without the development of negative metabolic effects.

Methods

Materials. DEX and dexamethasone-21-acetate were purchased from Sigma-Aldrich. All solvents were HPLC grade from Caledon Laboratories.

Animal experiments. WT, Lxr $\alpha^{-/-}$, Lxr $\beta^{-/-}$, and Lxr $\alpha/\beta^{-/-}$ mice (33, 34) were maintained on a mixed strain background (C57BL/6:129SvEv) and housed in a temperature and light-controlled environment. All mice used in the studies were male aged-matched between 3 and 8 months as indicated. The WT mice used in these studies were littermates derived from the original Lxr $\alpha/\beta^{-/-}$ crosses. For all the experiments described herein, the mice were bred homozygously, changing breeder pairs every 4 months to avoid fertility problems in the Lxr $\alpha/\beta^{-/-}$ mice. Mice were fed *ad libitum* the 2016S or 2018S diet from Harlan Teklad. To minimize the production of endogenous GCs from environmental stress, mice were sacrificed in the fed state (unless otherwise indicated) within 1 minute of initial handling by decapitation and within 2 hours after the start of the light cycle. Animals were treated with DEX or dexamethasone-21-acetate at 2.5 mg/kg in sesame oil (vehicle) twice daily for 5–7 days (s.c.) or 14 days (i.p.). From the different dosing regimens, it was determined that s.c. injections of DEX yielded higher intra-liver DEX levels compared with i.p. injections. There were only minor or insignificant changes in body weight after DEX treatment (Supplemental Table 1).



All animals were approved by the Faculty Advisory Committee on Animal Care at the University of Toronto and the Institutional Animal Care and Research Advisory Committee at the University of Texas Southwestern Medical Center.

Plasma analyses. Trunk blood was collected in EDTA tubes on ice, and plasma was stored at -80°C . Insulin and corticosterone levels were measured by RIA (Millipore). Blood glucose was measured using a handheld glucometer (FreeStyle) or after separation of plasma using the enzymatic kit from Wako. Free fatty acids were measured from plasma using an enzymatic assay (Wako).

Corticosterone and DEX LC/MS/MS analysis. Plasma corticosterone (Figure 1A) and liver DEX levels were measured by LC/MS/MS. Plasma samples (100 μl) were spiked with internal standard and precipitated with 4 volumes of acetonitrile. After centrifugation, the supernatant was washed with 100 μl of saturated KCl and 100 μl of water. The GCs were extracted in 4 volumes of 6:4 MTBE:CH₂Cl₂ and evaporated to dryness. Samples were resuspended in 250 μl of methanol for analysis. To the approximately 200 mg of liver (same piece that was used for triglyceride analysis), 84 ng of the internal standard triamcinolone acetonide was added prior to homogenization. After washing and measurement of cholesterol and triglyceride levels, as described above, the remaining sample was dried under N₂ and resuspended in 500 μl of methanol for analysis. Then, 10 μl was injected onto the LC/MS/MS triple quadrupole instrument (Agilent Technologies) running in ESI positive ion mode. Samples were loaded onto a Zorbax C18 column (4.6 \times 50 mm, 5 μm ; Agilent) and run using a mobile phase of methanol (MeOH) and water, both containing 5 mM ammonium acetate, increasing from 20% MeOH to 60% MeOH over 12 minutes, then flushing with 100% MeOH for 2 minutes before returning to initial conditions. Positive ions [M+H]⁺ for corticosterone (m/z 347 \rightarrow 329, RT 10.4 minutes), DEX (m/z 393 \rightarrow 373, RT 10.1 minutes), and triamcinolone acetonide (m/z 435 \rightarrow 415, RT 10.9 minutes) were monitored in multiple reaction monitoring mode.

Glucose and insulin tolerance tests. For the OGTT, mice were fasted 4 hours before receiving an oral gavage of 20% D-glucose (Sigma-Aldrich) (2 g/kg body weight). At 0, 15, 30, 60, and 120 minutes after injection, 20 μl of blood was collected from the tail into an EDTA-coated microvette tube. After centrifugation at 1500 g for 20 minutes, the plasma was stored at -80°C until glucose and insulin analysis. For the ITT, mice were fasted for 4 hours and given an i.p. injection of human insulin (0.75 U/kg; Sigma-Aldrich). At 0, 15, 30, 60, and 90 minutes, blood glucose was sampled from a tail nick as described above.

RNA isolation, cDNA synthesis, and real-time QPCR analysis. Total RNA was extracted from tissues using RNA STAT-60 (Tel-Test Inc.), treated with DNase I (RNase-free; Roche), and reverse transcribed into cDNA with random hexamers using the High Capacity Reverse Transcription System (ABI; Applied Biosystems). Primers used are shown in Supplemental Table 2 and were validated as previously described (79). Real-time quantitative PCR (QPCR) reactions were performed on an ABI 7900 in 384-well plates containing 12.5 ng cDNA, 150 nM of each primer, and 5 μl 2X SYBR Green PCR Master Mix (ABI) in a 10 μl total volume. Relative mRNA levels were calculated using the comparative Ct method normalized to cyclophilin mRNA.

Primary hepatocytes isolation. Mouse primary hepatocytes were isolated by collagenase perfusion and purified by centrifugation as described (80). Freshly prepared hepatocytes were seeded at a final density of 0.5×10^6 cells per well onto type I collagen-coated 6-well plates in attachment media (William's E Media, 10% charcoal stripped FBS, 1 \times penicillin/streptomycin, and 10 nM insulin). Media was exchanged 3 hours after plating, and all the experiments were performed on the second day. Ligands were added to the cells in M199 media without FBS, and cells were harvested 16 hours after ligand treatment for RNA extraction.

Western blot analysis. Protein extracts were subjected to SDS-PAGE and transferred to PVDF membranes. Membranes were incubated overnight at 4°C with primary polyclonal antibodies against Akt (1:1000; Cell Signaling Technologies), p-Akt (Ser473) (1:1000; Cell Signaling Technologies), GR (M-20, 1:200; Santa Cruz Biotechnology Inc.), or lamin B1 (1:1000; Abcam), followed by a 1-hour incubation with a peroxidase-conjugated anti-rabbit IgG (1:2000). Peroxidase activity was measured using ECL Plus (GE Healthcare) and visualized using the Storm phosphorimager (GE Healthcare). Quantitation was performed using ImageQuant from GE Healthcare.

ChIP. ChIP was carried out using the EZ ChIP kit (Millipore). Livers were perfused in situ for 30 minutes via the portal vein with either vehicle or 10 nM DEX. Whole liver was minced and cross-linked in 1% formaldehyde containing PBS, 1 mM DTT, and 1 mM PMSF for 10 minutes at room temperature. Cross-linking was stopped by addition of glycine to a final concentration of 125 mM for 5 minutes at room temperature, followed by centrifugation and washing the pellet twice in ice-cold PBS containing 1 mM DTT and protease inhibitors (Complete; Roche). Liver nuclei were recovered by Dounce homogenization in a hypotonic buffer (10 mM Hepes [pH 7.9], 1.5 mM MgCl₂, 10 mM KCl, 0.2% Nonidet P-40, 0.2 mM sodium orthovanadate, 0.15 mM spermine, 0.5 mM spermidine, 1 mM EDTA, 5% sucrose, 1 mM DTT, and protease inhibitor) and layered onto a cushion buffer (10 mM Tris-HCl [pH 7.5], 15 mM NaCl, 60 mM KCl, 0.15 mM spermine, 0.5 mM spermidine, 1 mM EDTA, 10% sucrose, 1 mM DTT, and protease inhibitor) followed by centrifugation. The nuclei pellet was washed with cold PBS and resuspended in 2 ml sonication buffer (0.75% SDS, 2 mM EDTA, and 50 mM Tris-HCl [pH 8.0]). The chromatin was sheared to 200–1000 bp by sonication. The sonicated chromatin was diluted 7.5-fold in dilution buffer (Millipore); 800 μl of diluted sample per immunoprecipitation was used. After 1-hour preclearing with protein G agarose beads (100 μl /IP), 10 μg of GR (M-20), SRC-1 (C-19), or C/EBP β (M-341) antibody (Santa Cruz Biotechnology Inc) was added for overnight incubation. Protein G agarose (60 μl) was used to recover the immune complexes (2 hours at 4°C). Washes and elutions were performed in accordance with the ChIP kit. DNA was reverse cross-linked overnight at 65°C , RNase treated for 30 minutes at 37°C , proteinase K treated for 2 hours at 45°C , and purified using a spin column to a final volume of 50 μl . The eluate was diluted 5-fold with water, and QPCR was performed using 5 μl of template DNA with the following primers: PEPCKpr GRE (0 kb) F, TGCAGCCAGCAACATATGAA, R, TGATGCAAACAGGCTCT; -3 kb PEPCKpr F, TGGGAGACACACATCT-TATTCCA, R, GTCCCTCTATAGACTTCCAGCACA; TAT GRE (-2.5 kb) F, CGCAAACAACAGGAAGCCTAA, R, CATGACACCCAAAAGCCTCTC. Quantitation was performed by QPCR (standard curve method) using serial dilutions of the input as standards.

Histology. Oil red O staining of liver sections was performed from formalin-fixed and sucrose-protected tissues. Cryosectioning and staining with oil red O was performed by the University of Texas Southwestern Medical Center Histology Core.

Liver triglycerides. Lipids were extracted from liver (0.2 g) in chloroform/methanol (2:1, v/v) using the Folch method (81). Extracts were washed once in 50 mM NaCl and twice in 0.36 M CaCl₂/methanol. The organic phase was separated and brought up to 5 ml with chloroform. Dried aliquots of standards and samples were redissolved in 10 μl of 1:1 chloroform/Triton X-100 and evaporated overnight. Samples were assayed for triglycerides using a commercial colorimetric assay (Thermo).

White blood cell differential. Blood (20 μl) was thinly smeared on a glass slide, air-dried, and dipped in Hemastain (Hema 3 stain set; Fisher). A differential count was then performed under brightfield microscopy on 100 white blood cells.



Thioglycolate-elicited peritoneal macrophages. Macrophages were collected by peritoneal lavage using 10 ml of PBS 4 days after i.p. injection of mice with 2 ml of 3% thioglycolate. Isolated cells were washed in PBS and pelleted at 1700 g. Cells were plated to a density of 2×10^6 cells/well in a 6-well plate in DMEM plus 10% FBS. After allowing the macrophages to adhere overnight, pretreatment with vehicle or 100 nM DEX was initiated in DMEM containing 10% charcoal stripped FBS. After 6 hours, wells were spiked with vehicle or LPS to a final concentration of 10 ng/ml and left an additional 18 hours before harvesting for RNA and QPCR.

Statistics. For comparison between 2 groups, the unpaired Student's *t* test was performed. One-way ANOVA followed by the Student-Newman-Keuls test was used to compare more than 2 groups. $P < 0.05$ was considered significant. All tests were performed using the software program Primer of Biostatistics (McGraw Hill).

Acknowledgments

We thank D. Ferguson for critically reading the manuscript and K. Gauthier, M. Hawkes, and J. Repa for their expert advice. This work was supported by the Howard Hughes Medical Institute

(to D.J. Mangelsdorf), the NIH (U19DK62434 to D.J. Mangelsdorf), the Robert A. Welch Foundation (I-1275 to D.J. Mangelsdorf), the Natural Sciences and Engineering Research Council of Canada (356873-08 to C.L. Cummins), the Canadian Institutes of Health Research (MOP-89361 and 97904 to C.L. Cummins), and the Canada Foundation for Innovation (to C.L. Cummins). M. Patel and L. Magomedova are supported by Ontario Graduate Scholarships. A.L. Bookout is supported by a predoctoral fellowship (GM007062). V. Lin is a Howard Hughes Medical Institute research associate, and D.J. Mangelsdorf is a Howard Hughes Medical Institute investigator.

Received for publication November 5, 2009, and accepted in revised form October 13, 2010.

Address correspondence to: Carolyn L. Cummins, University of Toronto, 144 College Street Rm. 1101, Toronto, Ontario M5S 3M2, Canada. Phone: 416.946.3466; Fax: 416.978.8511; E-mail: Carolyn.Cummins@utoronto.ca.

1. Lamb E. Top 200 prescription drugs of 2006. *Pharm Times*. 2007;2007-05-6472. <http://www.pharmacytimes.com/issue/pharmacy/2007/2007-05/2007-05-6472>. Accessed November 16, 2010.
2. Schimmer BP, Parker KL. Adrenocorticotropic hormone; adrenocortical steroids and their synthetic analogs; inhibitors of the synthesis and actions of adrenocortical hormones. In: Hardman JG, Limbird LE, eds. *Goodman & Gilman's The Pharmacological Basis of Therapeutics*. New York, New York, USA: McGraw-Hill; 2001:1649-1677.
3. Rosen J, Miner JN. The search for safer glucocorticoid receptor ligands. *Endocr Rev*. 2005;26(3):452-464.
4. Long CNH, Lukens FDW. The effects of adrenalectomy and hypophysectomy upon experimental diabetes in the cat. *J Exp Med*. 1936;63(4):465-469.
5. Andrew R, Gale CR, Walker BR, Seckl JR, Martyn CN. Glucocorticoid metabolism and the Metabolic Syndrome: associations in an elderly cohort. *Exp Clin Endocrinol Diabetes*. 2002;110(6):284-290.
6. Duclos M, Gatta B, Corcuff JB, Rashedi M, Pehourcq F, Roger P. Fat distribution in obese women is associated with subtle alterations of the hypothalamic-pituitary-adrenal axis activity and sensitivity to glucocorticoids. *Clin Endocrinol (Oxf)*. 2001;55(4):447-454.
7. Levitt NS, Lambert EV, Woods D, Hales CN, Andrew R, Seckl JR. Impaired glucose tolerance and elevated blood pressure in low birth weight, nonobese, young South African adults: early programming of cortisol axis. *J Clin Endocrinol Metab*. 2000;85(12):4611-4618.
8. Rask E, et al. Tissue-specific dysregulation of cortisol metabolism in human obesity. *J Clin Endocrinol Metab*. 2001;86(3):1418-1421.
9. Vegiopoulos A, Herzig S. Glucocorticoids, metabolism and metabolic diseases. *Mol Cell Endocrinol*. 2007;275(1-2):43-61.
10. Howlett TA, Rees LH, Besser GM. Cushing's syndrome. *Clin Endocrinol Metab*. 1985;14(4):911-945.
11. Shibli-Rahhal A, Van Beek M, Schlechte JA. Cushing's syndrome. *Clin Dermatol*. 2006;24(4):260-265.
12. Kotronen A, Seppala-Lindroos A, Bergholm R, Yki-Jarvinen H. Tissue specificity of insulin resistance in humans: fat in the liver rather than muscle is associated with features of the metabolic syndrome. *Diabetologia*. 2008;51(1):130-138.
13. Marchesini G, et al. Association of nonalcoholic fatty liver disease with insulin resistance. *Am J Med*. 1999;107(5):450-455.
14. Nguyen-Duy TB, Nichaman MZ, Church TS, Blair SN, Ross R. Visceral fat and liver fat are independent predictors of metabolic risk factors in men. *Am J Physiol Endocrinol Metab*. 2003;284(6):E1065-E1071.
15. Seppala-Lindroos A, et al. Fat accumulation in the liver is associated with defects in insulin suppression of glucose production and serum free fatty acids independent of obesity in normal men. *J Clin Endocrinol Metab*. 2002;87(7):3023-3028.
16. McMahon M, Gerich J, Rizza R. Effects of glucocorticoids on carbohydrate metabolism. *Diabetes Metab Rev*. 1988;4(1):17-30.
17. Sakoda H, et al. Dexamethasone-induced insulin resistance in 3T3-L1 adipocytes is due to inhibition of glucose transport rather than insulin signal transduction. *Diabetes*. 2000;49(10):1700-1708.
18. Weinstein SP, Wilson CM, Pritsker A, Cushman SW. Dexamethasone inhibits insulin-stimulated recruitment of GLUT4 to the cell surface in rat skeletal muscle. *Metabolism*. 1998;47(1):3-6.
19. Divertie GD, Jensen MD, Miles JM. Stimulation of lipolysis in humans by physiological hypercortisolemia. *Diabetes*. 1991;40(10):1228-1232.
20. Hasselgren PO. Glucocorticoids and muscle catabolism. *Curr Opin Clin Nutr Metab Care*. 1999;2(3):201-205.
21. Delaunay F, et al. Pancreatic beta cells are important targets for the diabetogenic effects of glucocorticoids. *J Clin Invest*. 1997;100(8):2094-2098.
22. Gross KL, Cidlowski JA. Tissue-specific glucocorticoid action: a family affair. *Trends Endocrinol Metab*. 2008;19(9):331-339.
23. Kalaany NY, Mangelsdorf DJ. LXRS AND FXR: The yin and yang of cholesterol and fat metabolism. *Annu Rev Physiol*. 2006;68:159-191.
24. Bookout AL, Jeong Y, Downes M, Yu RT, Evans RM, Mangelsdorf DJ. Anatomical profiling of nuclear receptor expression reveals a hierarchical transcriptional network. *Cell*. 2006;126(4):789-799.
25. Hanson RW, Reshef L. Regulation of phosphoenolpyruvate carboxykinase (GTP) gene expression. *Annu Rev Biochem*. 1997;66:581-611.
26. van Schaftingen E, Gerin I. The glucose-6-phosphatase system. *Biochem J*. 2002;362(pt 3):513-532.
27. Janowski BA, et al. Structural requirements of ligands for the oxysterol liver X receptors LXRA and LXR-beta. *Proc Natl Acad Sci U S A*. 1999;96(1):266-271.
28. Janowski BA, Willy PJ, Devi TR, Falck JR, Mangelsdorf DJ. An oxysterol signalling pathway mediated by the nuclear receptor LXR alpha. *Nature*. 1996;383(6602):728-731.
29. Costet P, Luo Y, Wang N, Tall AR. Sterol-dependent transactivation of the ABC1 promoter by the liver X receptor/retinoid X receptor. *J Biol Chem*. 2000;275(36):28240-28245.
30. Repa JJ, Berge KE, Pomajzl C, Richardson JA, Hobbs H, Mangelsdorf DJ. Regulation of ATP-binding cassette transporters ABCG5 and ABCG8 by the liver X receptors alpha and beta. *J Biol Chem*. 2002;277(21):18793-18800.
31. Venkateswaran A, Repa JJ, Lobaccaro JM, Bronson A, Mangelsdorf DJ, Edwards PA. Human white/murine ABC8 mRNA levels are highly induced in lipid-loaded macrophages. A transcriptional role for specific oxysterols. *J Biol Chem*. 2000;275(19):14700-14707.
32. Lehmann JM, et al. Activation of the nuclear receptor LXR by oxysterols defines a new hormone response pathway. *J Biol Chem*. 1997;272(6):3137-3140.
33. Peet DJ, et al. Cholesterol and bile acid metabolism are impaired in mice lacking the nuclear oxysterol receptor LXR alpha. *Cell*. 1998;93(5):693-704.
34. Repa JJ, et al. Regulation of mouse sterol regulatory element-binding protein-1c gene (SREBP-1c) by oxysterol receptors, LXRA and LXRbeta. *Genes Dev*. 2000;14(22):2819-2830.
35. Ogawa S, et al. Molecular determinants of crosstalk between nuclear receptors and toll-like receptors. *Cell*. 2005;122(5):707-721.
36. Zelcer N, Tontonoz P. Liver X receptors as integrators of metabolic and inflammatory signaling. *J Clin Invest*. 2006;116(3):607-614.
37. Cao G, et al. Antidiabetic action of a liver x receptor agonist mediated by inhibition of hepatic gluconeogenesis. *J Biol Chem*. 2003;278(2):1131-1136.
38. Laffitte BA, et al. Activation of liver X receptor improves glucose tolerance through coordinate regulation of glucose metabolism in liver and adipose tissue. *Proc Natl Acad Sci U S A*. 2003;100(9):5419-5424.
39. Grefhorst A, et al. Differential effects of pharmacological liver X receptor activation on hepatic and peripheral insulin sensitivity in lean and ob/ob mice. *Am J Physiol Endocrinol Metab*. 2005;289(5):E829-E838.
40. Stulnig TM, Oppermann U, Steffensen KR, Schuster GU, Gustafsson JA. Liver X receptors downregulate 11beta-hydroxysteroid dehydrogenase type 1 expression and activity. *Diabetes*. 2002;51(8):2426-2433.
41. Dalen KT, Ulven SM, Bamberg K, Gustafsson JA, Nebb HI. Expression of the insulin-responsive glucose transporter GLUT4 in adipocytes is dependent on liver X receptor alpha. *J Biol Chem*. 2003;278(48):48283-48291.
42. Cummins CL, et al. Liver X receptors regulate adrenal cholesterol balance. *J Clin Invest*. 2006;116(7):1902-1912.
43. Kalaany NY, et al. LXRs regulate the balance between fat storage and oxidation. *Cell Metab*. 2005;1(4):231-244.



44. Guillaume-Gentil C, Assimacopoulos-Jeanneret F, Jeanrenaud B. Involvement of non-esterified fatty acid oxidation in glucocorticoid-induced peripheral insulin resistance in vivo in rats. *Diabetologia*. 1993;36(10):899–906.
45. Jantzen HM, et al. Cooperativity of glucocorticoid response elements located far upstream of the tyrosine aminotransferase gene. *Cell*. 1987;49(1):29–38.
46. Schmid E, Schmid W, Jantzen M, Mayer D, Jastorff B, Schutz G. Transcription activation of the tyrosine aminotransferase gene by glucocorticoids and cAMP in primary hepatocytes. *Eur J Biochem*. 1987;165(3):499–506.
47. Alberti S, et al. Hepatic cholesterol metabolism and resistance to dietary cholesterol in LXRbeta-deficient mice. *J Clin Invest*. 2001;107(5):565–573.
48. Repa JJ, Mangelsdorf DJ. The role of orphan nuclear receptors in the regulation of cholesterol homeostasis. *Annu Rev Cell Dev Biol*. 2000;16:459–481.
49. Tobin KA, et al. Liver X receptors as insulin-mediating factors in fatty acid and cholesterol biosynthesis. *J Biol Chem*. 2002;277(12):10691–10697.
50. Zhang Y, Repa JJ, Gauthier K, Mangelsdorf DJ. Regulation of lipoprotein lipase by the oxysterol receptors, LXRalpha and LXRbeta. *J Biol Chem*. 2001;276(46):43018–43024.
51. Gerin I, et al. LXRbeta is required for adipocyte growth, glucose homeostasis, and beta cell function. *J Biol Chem*. 2005;280(24):23024–23031.
52. Altman KI, Miller LL, Bly CG. The synergistic effect of cortisone and insulin on lipogenesis in the perfused rat liver as studied with alpha-C14-acetate. *Arch Biochem*. 1951;31(2):329–331.
53. Diamant S, Shafir E. Modulation of the activity of insulin-dependent enzymes of lipogenesis by glucocorticoids. *Eur J Biochem*. 1975;53(2):541–546.
54. Joseph SB, et al. LXR-dependent gene expression is important for macrophage survival and the innate immune response. *Cell*. 2004;119(2):299–309.
55. Joseph SB, Castrillo A, Laffitte BA, Mangelsdorf DJ, Tontonoz P. Reciprocal regulation of inflammation and lipid metabolism by liver X receptors. *Nat Med*. 2003;9(2):213–219.
56. Korf H, et al. Liver X receptors contribute to the protective immune response against *Mycobacterium tuberculosis* in mice. *J Clin Invest*. 2009;119(6):1626–1637.
57. Hall RK, Sladek FM, Granner DK. The orphan receptors COUP-TF and HNF-4 serve as accessory factors required for induction of phosphoenolpyruvate carboxykinase gene transcription by glucocorticoids. *Proc Natl Acad Sci U S A*. 1995;92(2):412–416.
58. Imai E, Miner JN, Mitchell JA, Yamamoto KR, Granner DK. Glucocorticoid receptor-cAMP response element-binding protein interaction and the response of the phosphoenolpyruvate carboxykinase gene to glucocorticoids. *J Biol Chem*. 1993;268(8):5353–5356.
59. Wang JC, Stromstedt PE, Sugiyama T, Granner DK. The phosphoenolpyruvate carboxykinase gene glucocorticoid response unit: identification of the functional domains of accessory factors HNF3 beta (hepatic nuclear factor-3 beta) and HNF4 and the necessity of proper alignment of their cognate binding sites. *Mol Endocrinol*. 1999;13(4):604–618.
60. Park EA, et al. The role of the CCAAT/enhancer-binding protein in the transcriptional regulation of the gene for phosphoenolpyruvate carboxykinase (GTP). *Mol Cell Biol*. 1990;10(12):6264–6272.
61. Chakravarty K, Cassuto H, Reshef L, Hanson RW. Factors that control the tissue-specific transcription of the gene for phosphoenolpyruvate carboxykinase-C. *Crit Rev Biochem Mol Biol*. 2005;40(3):129–154.
62. Chakravarty K, Hanson RW. Insulin regulation of phosphoenolpyruvate carboxykinase-c gene transcription: the role of sterol regulatory element-binding protein 1c. *Nutr Rev*. 2007;65(6 pt 2):S47–S56.
63. Hall RK, Wang XL, George L, Koch SR, Granner DK. Insulin represses phosphoenolpyruvate carboxykinase gene transcription by causing the rapid disruption of an active transcription complex: a potential epigenetic effect. *Mol Endocrinol*. 2007;21(2):550–563.
64. Cassuto H, et al. Glucocorticoids regulate transcription of the gene for phosphoenolpyruvate carboxykinase in the liver via an extended glucocorticoid regulatory unit. *J Biol Chem*. 2005;280(40):33873–33884.
65. Puigserver P, et al. Insulin-regulated hepatic gluconeogenesis through FOXO1-PGC-1alpha interaction. *Nature*. 2003;423(6939):550–555.
66. Letteron P, Brahimi-Bourouina N, Robin MA, Moreau A, Feldmann G, Pessayre D. Glucocorticoids inhibit mitochondrial matrix acyl-CoA dehydrogenases and fatty acid beta-oxidation. *Am J Physiol*. 1997;272(5 pt 1):G1141–1150.
67. Lemke U, et al. The glucocorticoid receptor controls hepatic dyslipidemia through Hes1. *Cell Metab*. 2008;8(3):212–223.
68. Inagaki T, et al. Endocrine regulation of the fasting response by PPARalpha-mediated induction of fibroblast growth factor 21. *Cell Metab*. 2007;5(6):415–425.
69. Bernal-Mizrachi C, et al. Dexamethasone induction of hypertension and diabetes is PPAR-alpha dependent in LDL receptor-null mice. *Nat Med*. 2003;9(8):1069–1075.
70. Matsusue K, et al. Hepatic steatosis in leptin-deficient mice is promoted by the PPARgamma target gene Fsp27. *Cell Metab*. 2008;7(4):302–311.
71. Shimano H, Horton JD, Shimomura I, Hammer RE, Brown MS, Goldstein JL. Isoform 1c of sterol regulatory element binding protein is less active than isoform 1a in livers of transgenic mice and in cultured cells. *J Clin Invest*. 1997;99(5):846–854.
72. Schultz JR, et al. Role of LXRs in control of lipogenesis. *Genes Dev*. 2000;14(22):2831–2838.
73. Miner JN, Yamamoto KR. The basic region of AP-1 specifies glucocorticoid receptor activity at a composite response element. *Genes Dev*. 1992;6(12B):2491–2501.
74. Nissen RM, Yamamoto KR. The glucocorticoid receptor inhibits NFkappaB by interfering with serine-2 phosphorylation of the RNA polymerase II carboxy-terminal domain. *Genes Dev*. 2000;14(18):2314–2329.
75. De Bosscher K, Haegeman G. Minireview: latest perspectives on antiinflammatory actions of glucocorticoids. *Mol Endocrinol*. 2009;23(3):281–291.
76. Schacke H, Docke WD, Asadullah K. Mechanisms involved in the side effects of glucocorticoids. *Pharmacol Ther*. 2002;96(1):23–43.
77. Schacke H, et al. Dissociation of transactivation from transrepression by a selective glucocorticoid receptor agonist leads to separation of therapeutic effects from side effects. *Proc Natl Acad Sci U S A*. 2004;101(1):227–232.
78. Schacke H, Berger M, Rehwinkel H, Asadullah K. Selective glucocorticoid receptor agonists (SEGRAs): novel ligands with an improved therapeutic index. *Mol Cell Endocrinol*. 2007;275(1–2):109–117.
79. Bookout AL, Cummins CL, Mangelsdorf DJ, Pesola JM, Kramer MF. High-throughput real-time quantitative reverse transcription PCR. *Curr Protoc Mol Biol*. 2006;Chapter 15:Unit 15.8.
80. Horton JD, Shimano H, Hamilton RL, Brown MS, Goldstein JL. Disruption of LDL receptor gene in transgenic SREBP-1a mice unmasks hyperlipidemia resulting from production of lipid-rich VLDL. *J Clin Invest*. 1999;103(7):1067–1076.
81. Folch J, Lees M, Sloane Stanley GH. A simple method for the isolation and purification of total lipides from animal tissues. *J Biol Chem*. 1957;226(1):497–509.